

## SUPPORTING INFORMATION

# **Synthesis of *brookite* TiO<sub>2</sub> nanorods with isolated Co(II) surface sites and photocatalytic degradation of 5,8-dihydroxy-1,4-naphthoquinone dye**

Wonjun Kang,<sup>1</sup> Charles S. Spanjers,<sup>2</sup> Robert M. Rioux,<sup>2\*</sup> James D. Hoefelmeyer<sup>1\*</sup>

<sup>1</sup>Department of Chemistry, University of South Dakota, 414 E. Clark St., Vermillion, SD 57069

<sup>2</sup>Department of Chemical Engineering, The Pennsylvania State University, 165 Fenske Laboratory, University Park, PA 16802-4400

Corresponding author email: James.Hoefelmeyer@usd.edu, rioux@engr.psu.edu

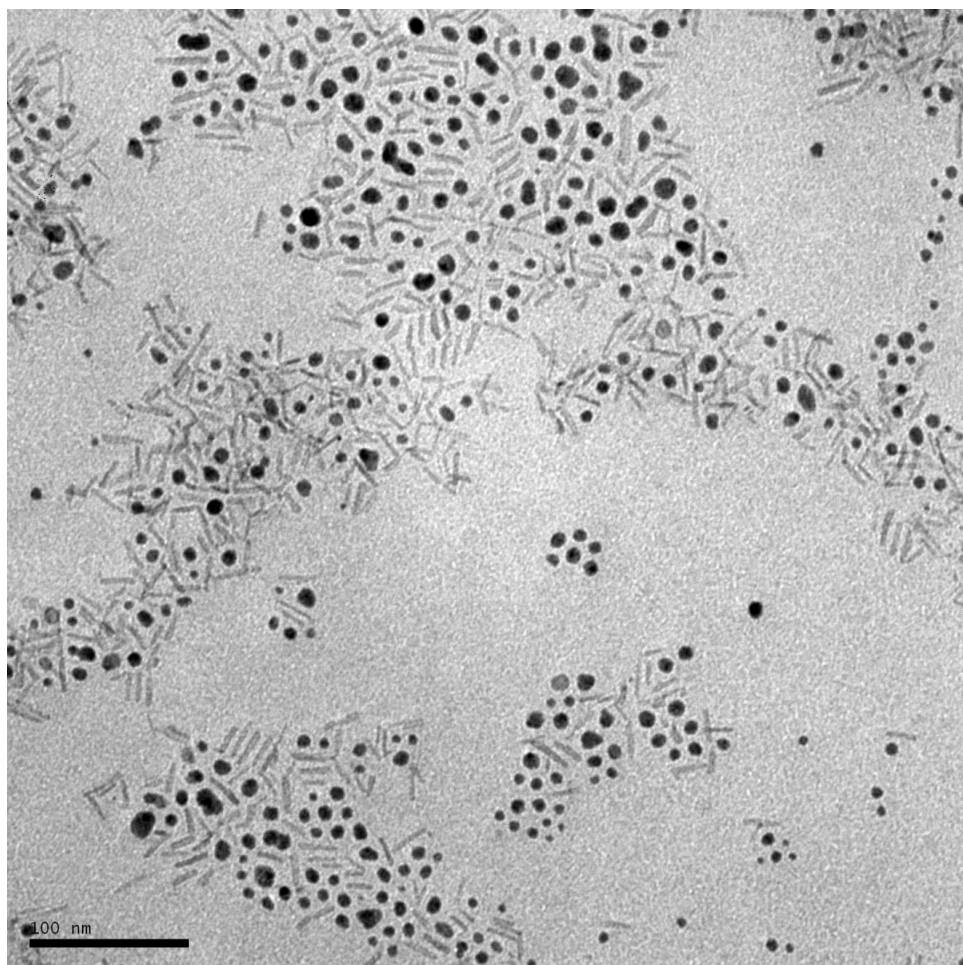


**Figure S1.** TEM image of dispersion of  $\text{TiO}_2$  NR and Co NPs typically formed via decomposition of  $\text{Co}_2(\text{CO})_8$  in the presence of  $\text{TiO}_2$  NR under the reaction conditions reported by Casavola et al.[1].

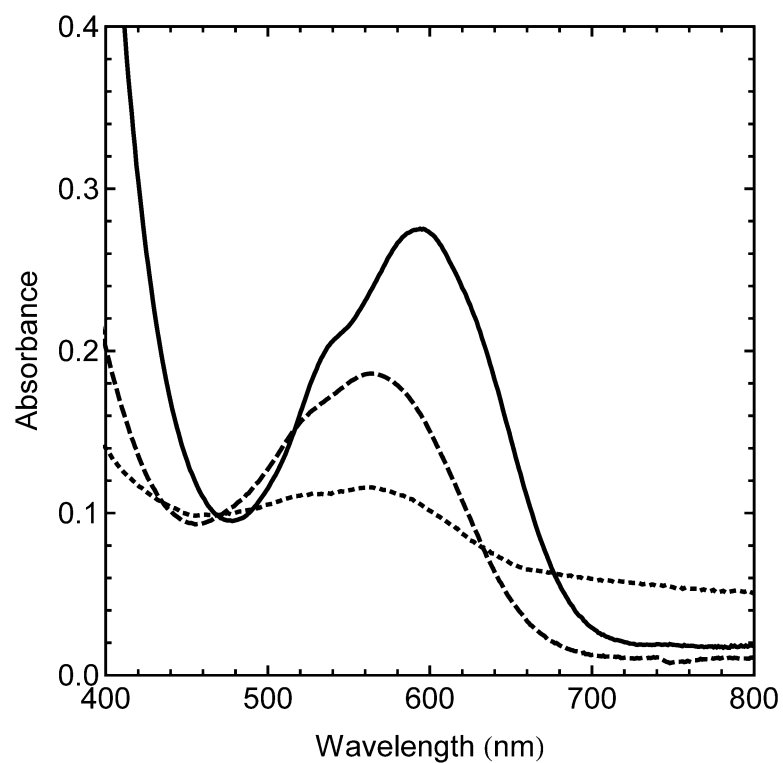


**Figure S2.** UV-visible spectrum of pink supernatant upon decomposition of  $\text{Co}_2(\text{CO})_8$  in the absence of  $\text{TiO}_2$  NR (---), pink supernatant separated from the dispersion of Co(II)- $\text{TiO}_2$  NR (—), and blue Co(II)- $\text{TiO}_2$  dispersion (—).

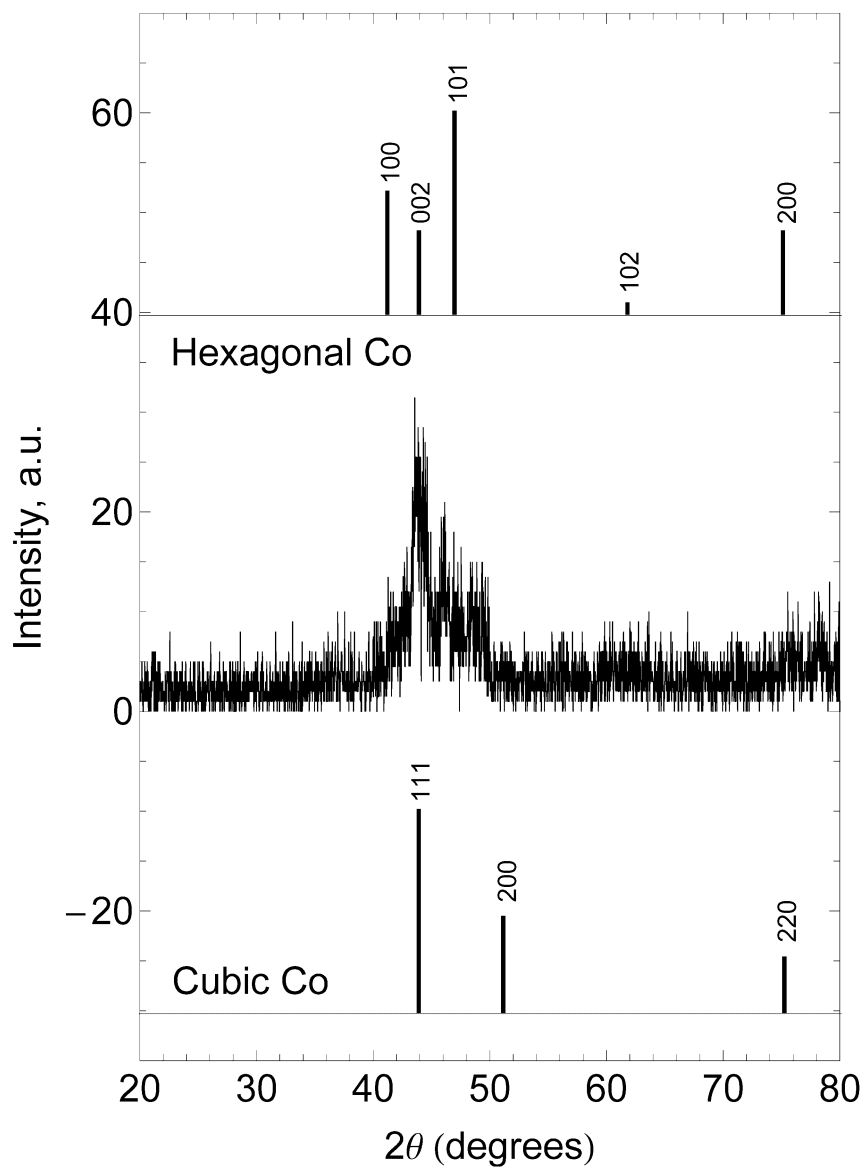


**Figure S3.** Powder XRD data of the highly amorphous cobalt precipitate formed during synthesis of Co(II)-TiO<sub>2</sub> NRs.

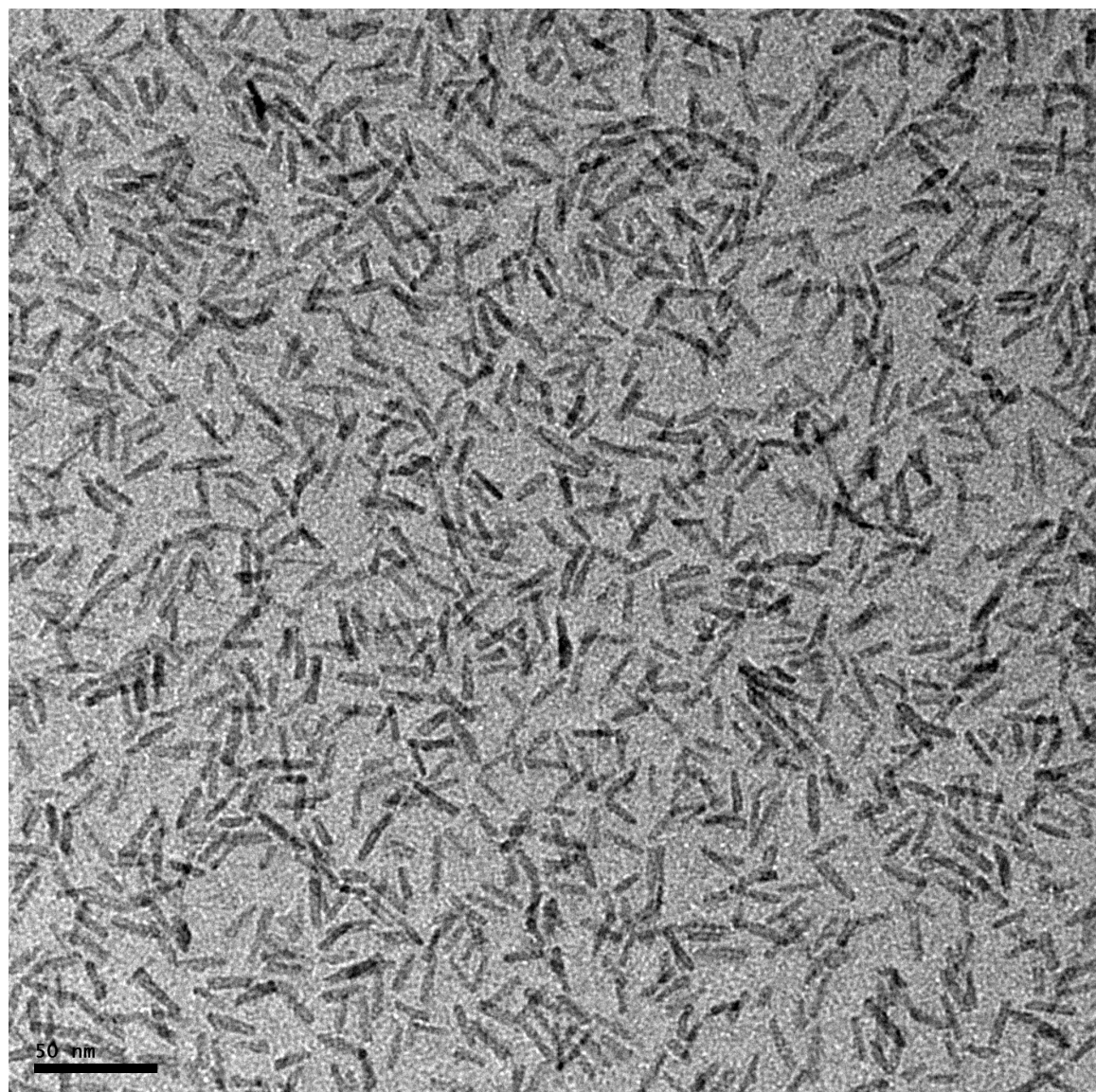


**Figure S4.** TEM image of Co(II)-TiO<sub>2</sub> NR.

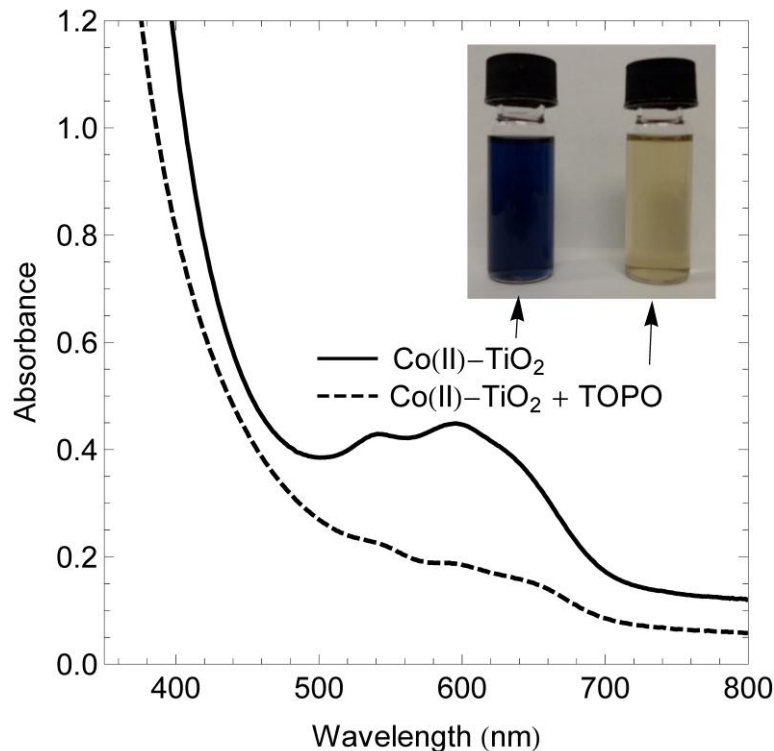


**Figure S5.** Photographs and UV-visible spectra of  $\text{Co(II)-TiO}_2$  NRs before and after treatment with trioctylphosphine oxide. The  $\text{Co(II)-TiO}_2$  NR dispersion is blue and shows prominent absorbance feature at 600 nm. After treatment with trioctylphosphine oxide at  $250^\circ\text{C}$  for 14 hours, much of the cobalt was removed from the nanorods and into the supernatant. Precipitation of the nanorods allowed separation of the supernatant. The nanorods ( $\text{Co(II)-TiO}_2 + \text{TOPO}$ ) redispersed in hexanes and were pale yellow, having lost  $\sim 70\%$  of the cobalt content. The UV-visible spectrum shows greatly reduced absorbance features from cobalt(II).

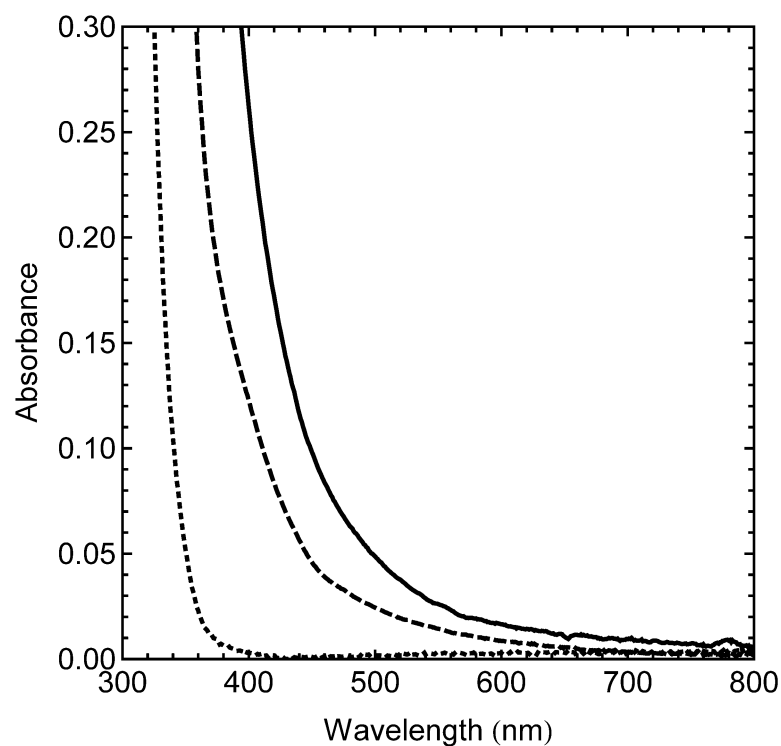


**Figure S6.** UV-visible spectra of TiO<sub>2</sub> NR (---), Co(II)-TiO<sub>2</sub> treated with DMG (—), and TiO<sub>2</sub> treated with DMG (—).

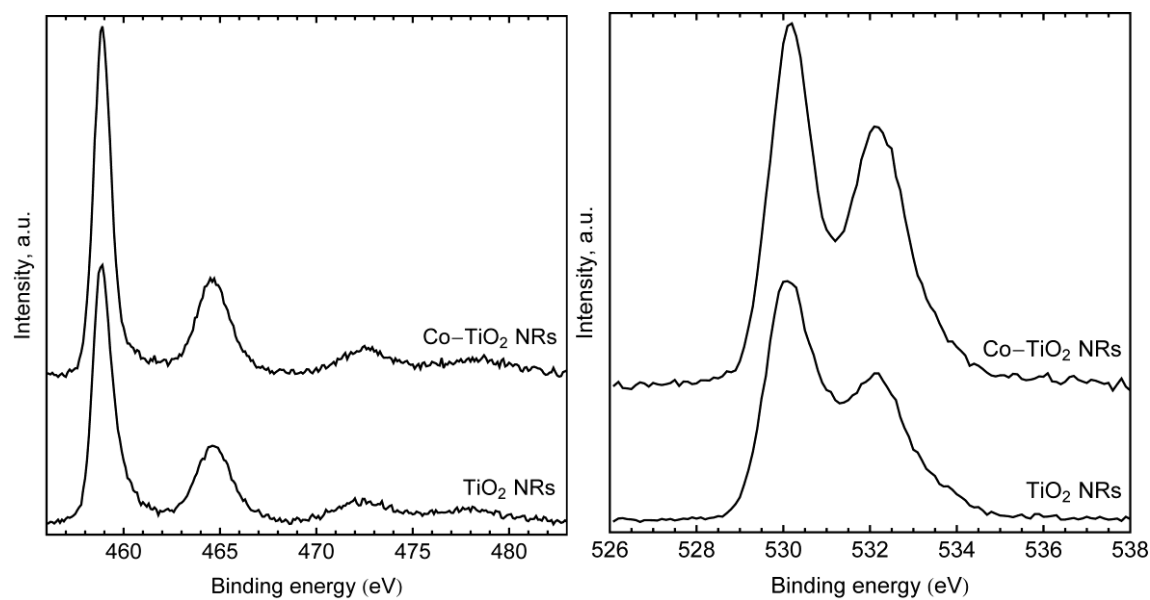


**Figure S7.** Ti 2p (left) and O 1s (right) XPS data of TiO<sub>2</sub> NR and Co(II)-TiO<sub>2</sub> NR.

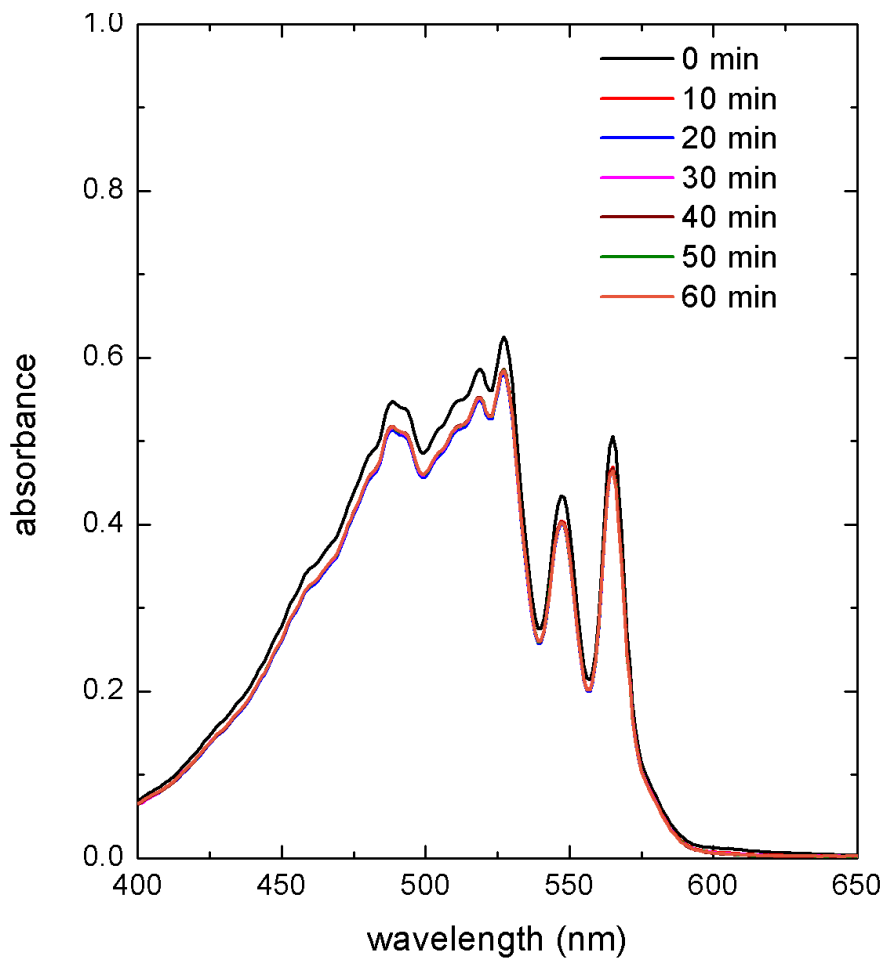


**Figure S8.** UV-visible spectra of DHNQ under visible light irradiation at room temperature in hexane. Spectra were recorded in 10-minute intervals. The dye concentration at 0 min was  $99.9 \pm 5.3 \mu\text{M}$ . The extinction coefficient,  $\epsilon = 7.0 \times 10^3 \pm 0.4 \times 10^3 \text{ M}^{-1}\text{cm}^{-1}$  at  $\lambda_{\text{max}} = 527\text{nm}$ .

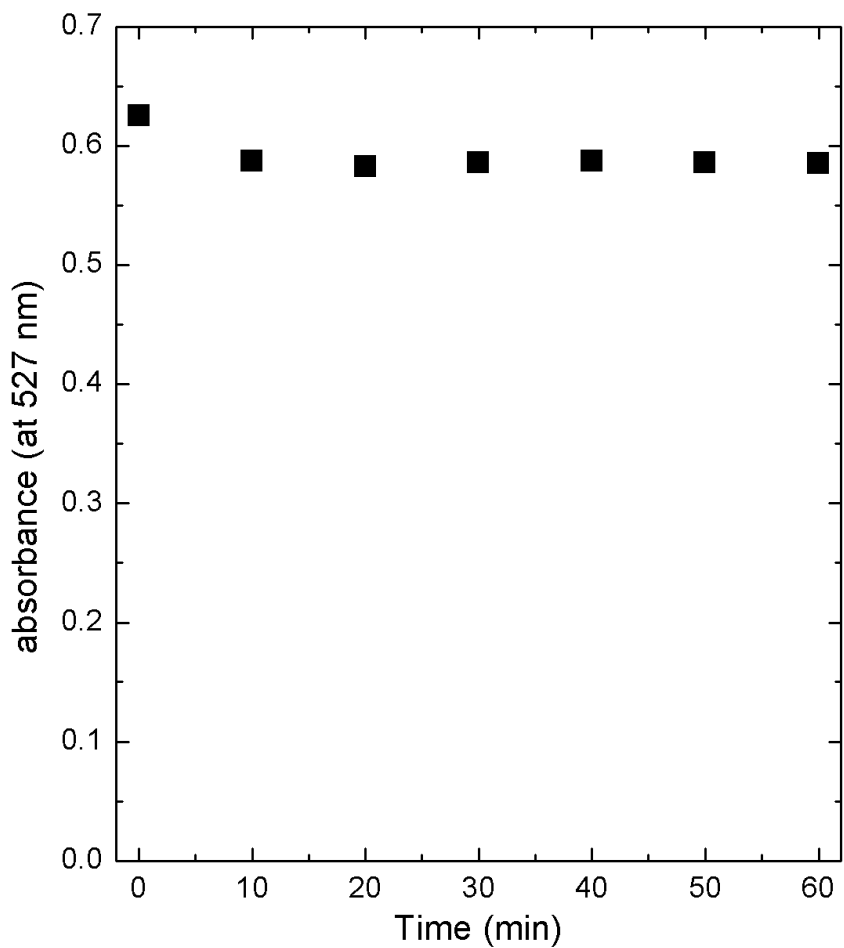


**Figure S9.** Time-dependent absorption of DHNQ dye at  $\lambda=527\text{nm}$  in hexane at room temperature. The dye concentration at 0 min was  $99.9 \pm 5.3 \mu\text{M}$ . Absorbance data from Figure S2.

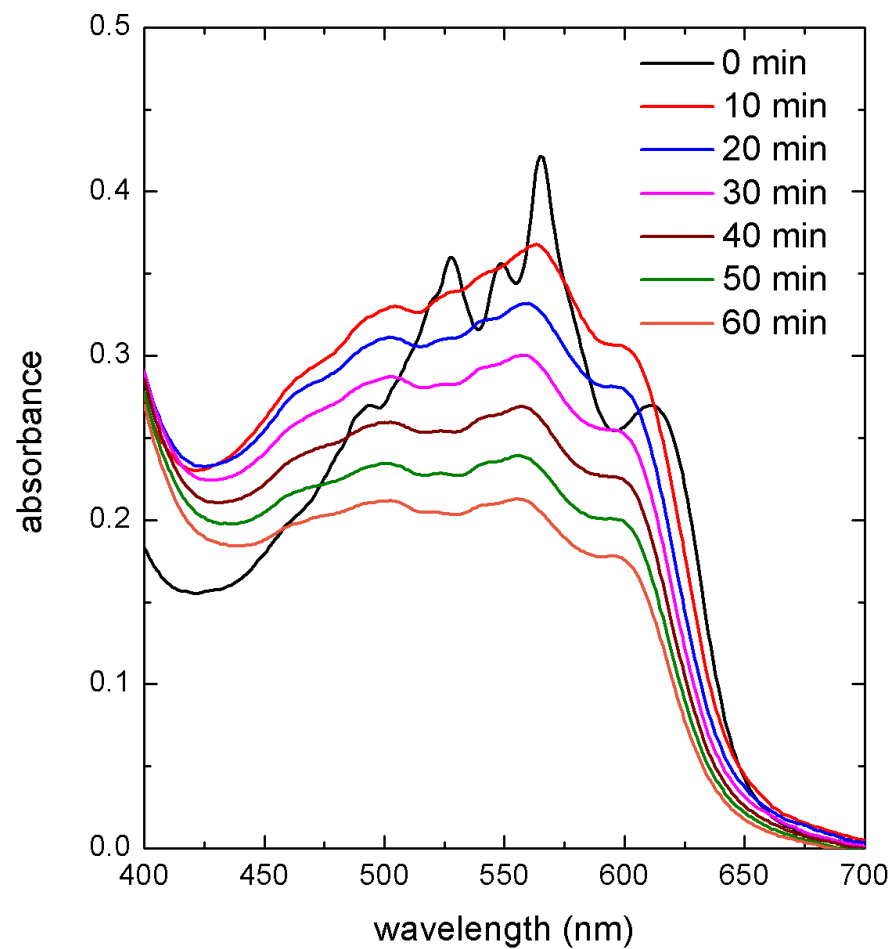


**Figure S10.** UV-visible spectra of DHNQ + TiO<sub>2</sub> NR under visible light irradiation at room temperature in hexane. Spectra were recorded in 10-minute intervals. At zero minutes, the spectrum resembles the spectrum of free DHNQ. The spectra afterward are presumed to be the adsorbed molecule on TiO<sub>2</sub> NR. The local absorbance maximum,  $\lambda = 502$  nm has a measured extinction coefficient,  $\epsilon = 4.0 \times 10^3 \pm 0.2 \times 10^3 \text{ M}^{-1}\text{cm}^{-1}$ .

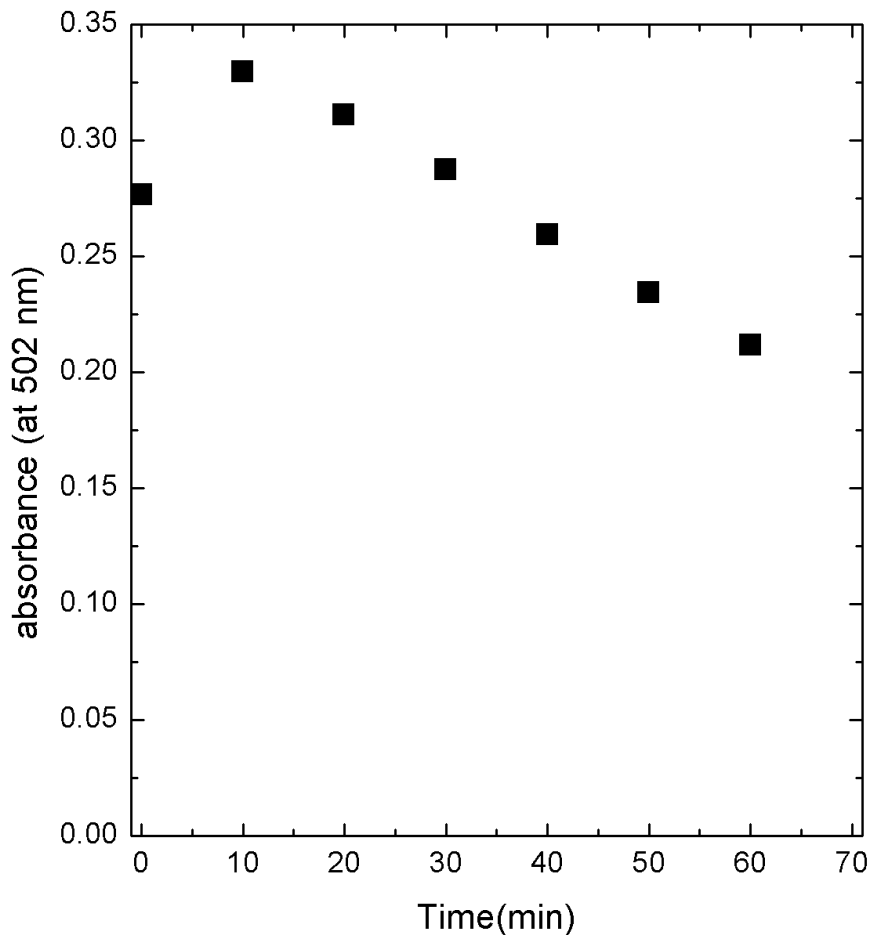


**Figure S11.** Time-dependent absorbance of DHNQ in the presence of  $\text{TiO}_2$  NRs at  $\lambda = 502$  nm in hexane at room temperature. The absorbance was determined by subtracting the spectrum of the  $\text{TiO}_2$  NRs from each spectra in Figure S4. The slope of the absorbance data from  $t = 10$ -60 minutes was used to determine the absorbance at  $t = 0$ . From a linear regression analysis, the equation,  $\text{absorbance} = -2.4 \times 10^{-3}(t) + 0.357$  fit the data with a correlation coefficient,  $R^2$  of 0.997.

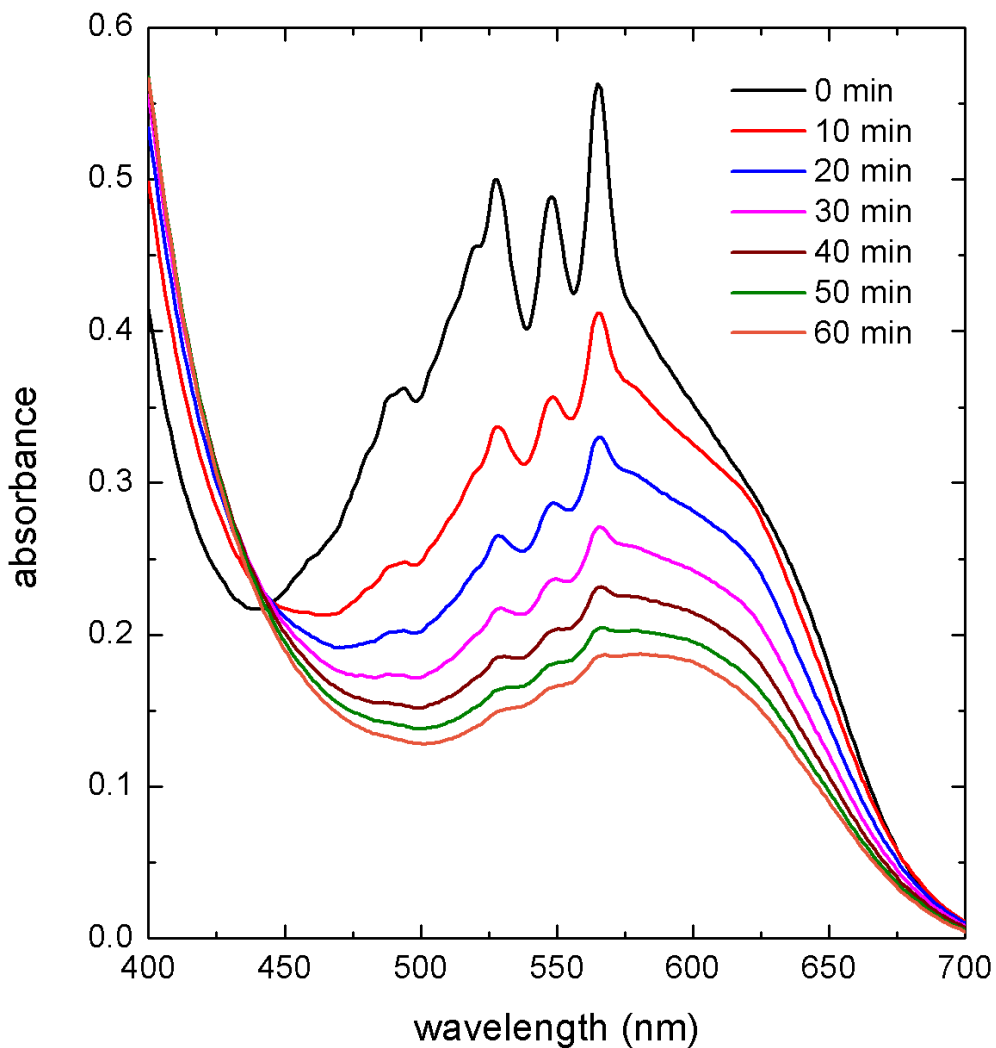


**Figure S12.** UV-visible spectra of DHNQ + Co(II)-TiO<sub>2</sub> NR under visible light irradiation at room temperature in hexane. Spectra were recorded in 10-minute intervals. The transition ( $\lambda_{\text{max}} = 565 \text{ nm}$ ) is superimposed with the Co(II) d-d transitions from the Co(II)-TiO<sub>2</sub> NRs. Subtraction of the Co(II)-TiO<sub>2</sub> NR spectrum yields an extinction coefficient,  $\epsilon \approx 4.3 \times 10^3 \pm 0.2 \times 10^3 \text{ M}^{-1} \text{cm}^{-1}$ .

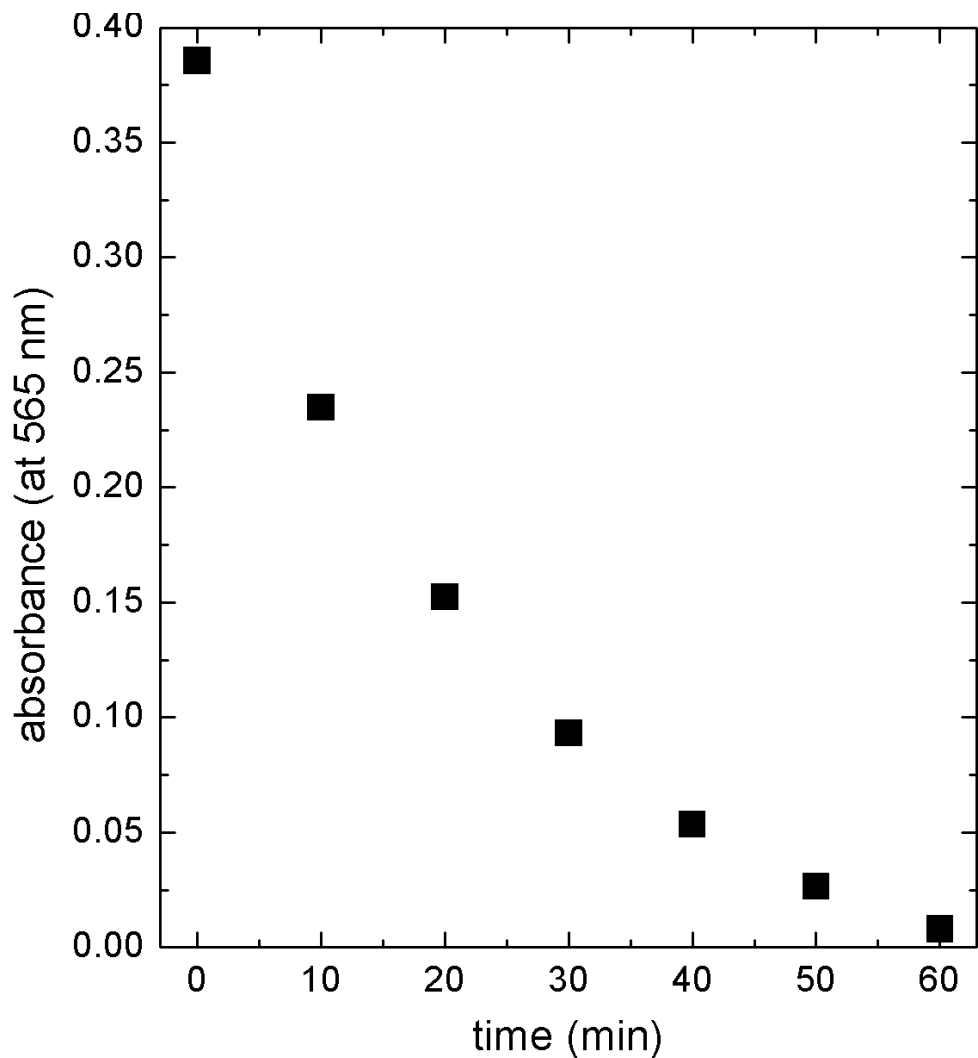


**Figure S13.** Time-dependent absorbance of DHNQ in the presence of Co(II)- $\text{TiO}_2$  NRs at  $\lambda = 565$  nm in hexane at room temperature. The absorbance was determined by subtracting the spectrum of the Co(II)- $\text{TiO}_2$  NRs from each spectra in Figure S6.

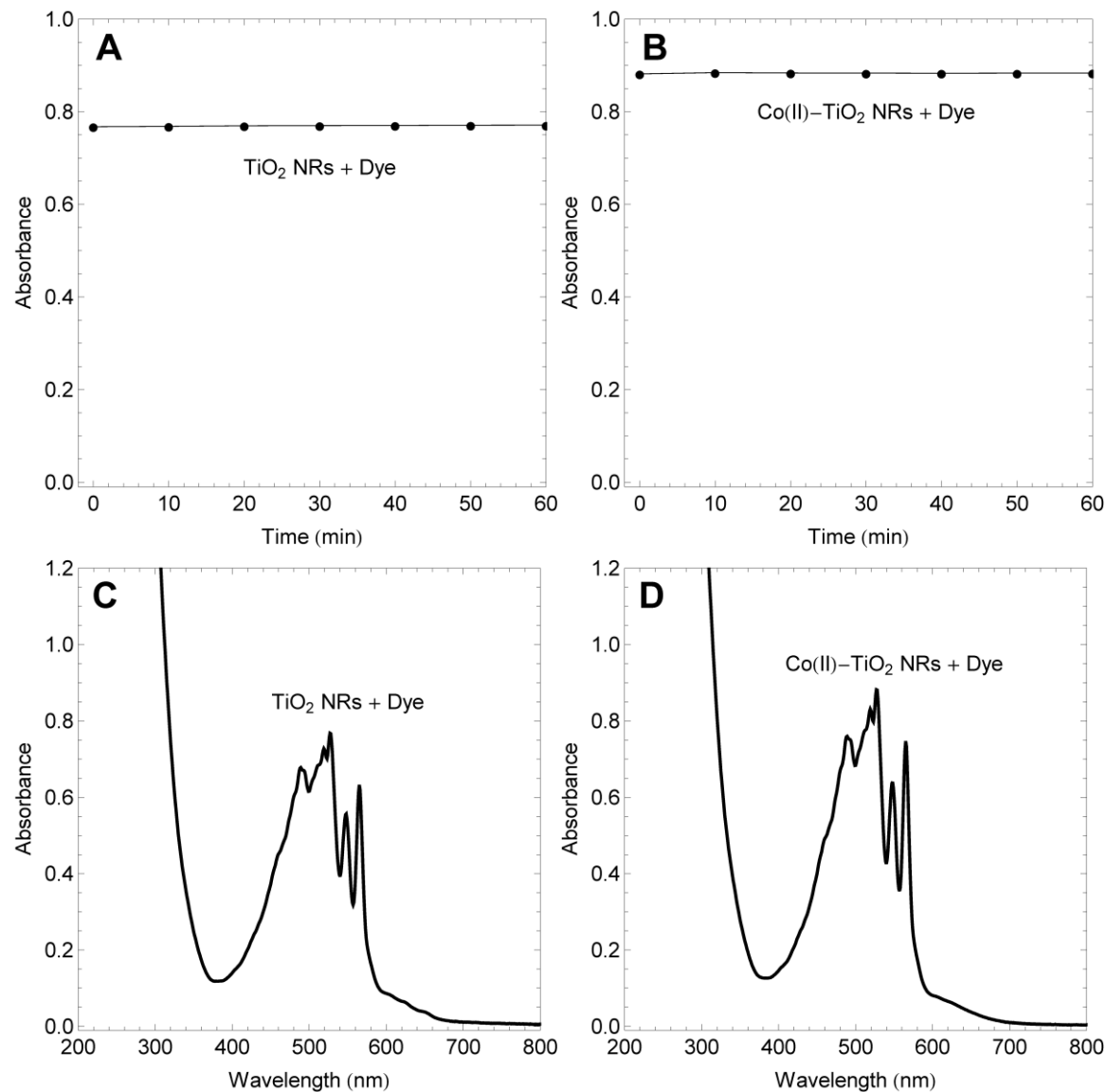


**Figure S14.** Top left: Absorbance versus time for  $\text{TiO}_2$  + DHNQ in the dark. Bottom left: UV-visible spectra of  $\text{TiO}_2$  + DHNQ in the dark. Top right: Absorbance versus time for  $\text{Co}(\text{II})-\text{TiO}_2$  + DHNQ in the dark. Bottom left: UV-visible spectra of  $\text{Co}(\text{II})-\text{TiO}_2$  + DHNQ in the dark.

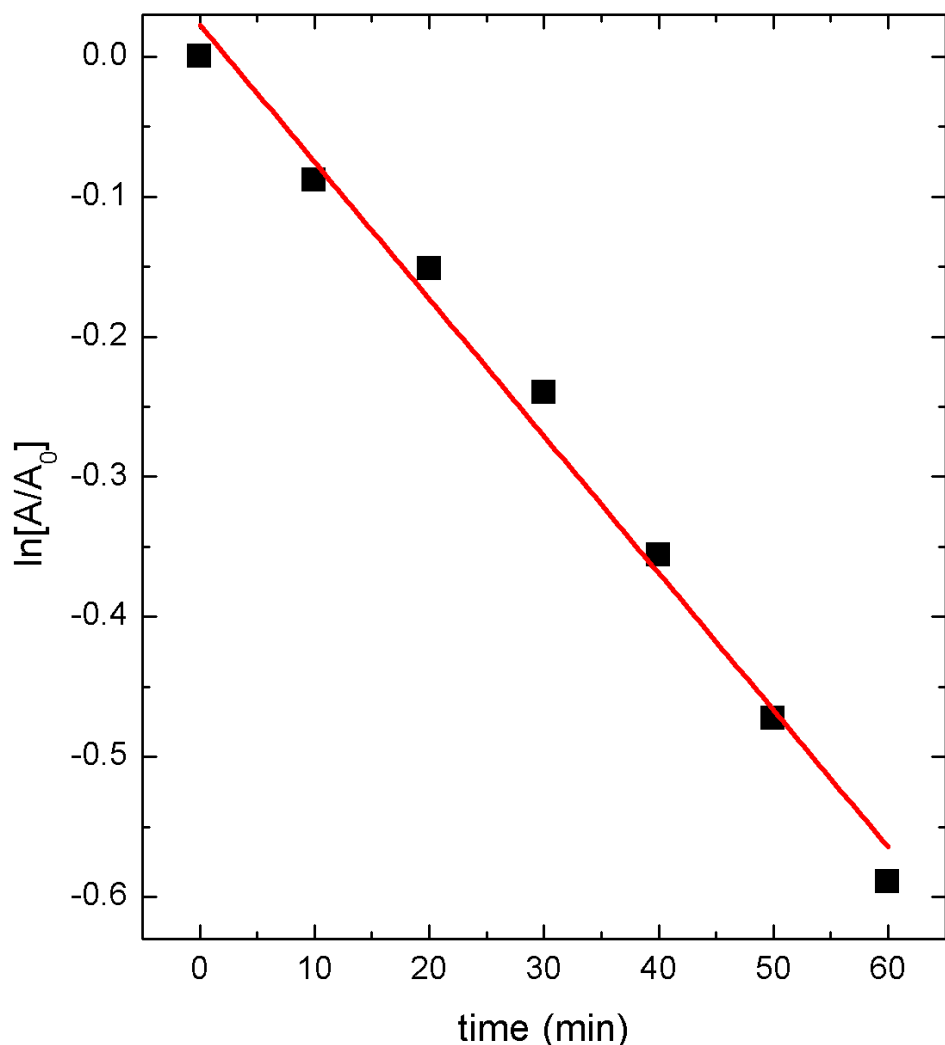


**Figure S15.** Linear plot of normalized absorbance versus time for DHNQ + TiO<sub>2</sub> at room temperature in hexane. From a linear regression analysis, the equation,  $\ln[A/A_0] = -0.0098(t) + 0.0227$  fit the data with a correlation coefficient,  $R^2$  of 0.98917.

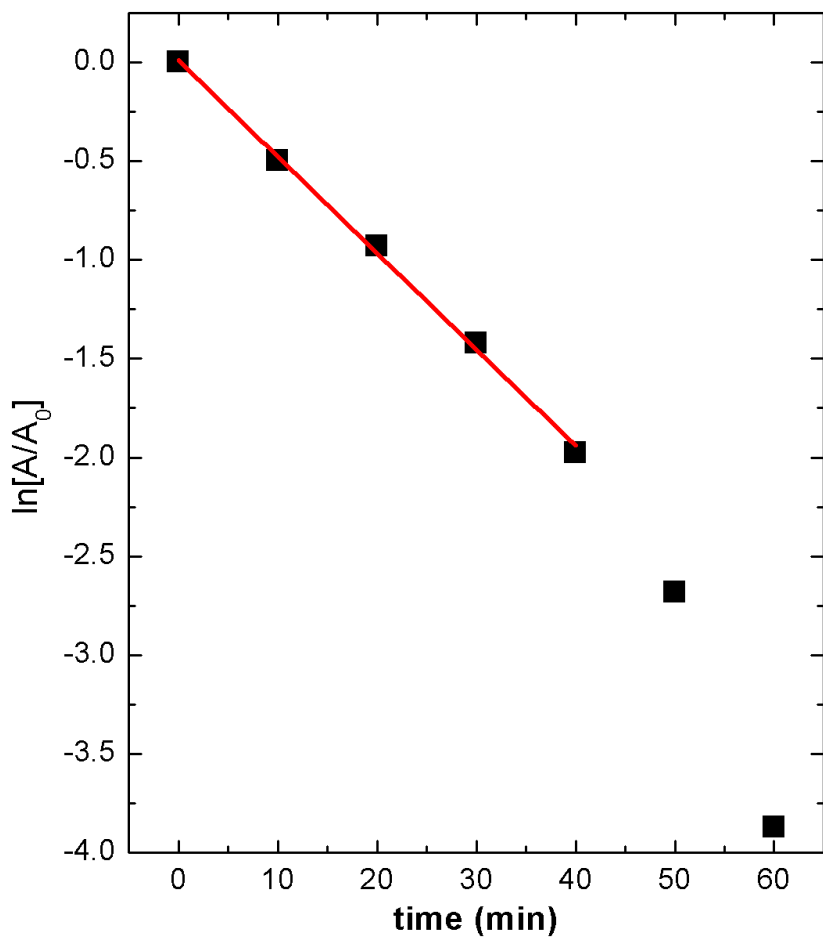


**Figure S16.** Linear plot of normalized absorbance versus time for DHNQ + Co(II)-TiO<sub>2</sub>. From the linear regression analysis, the equation,  $\ln[A/A_0] = -0.0488(t) + 0.0112$  fit the data with a correlation coefficient,  $R^2$  of 0.99825 over the time interval 0-40 minutes. The last two data points were discarded because the data was obtained by subtracting the absorbance of Co(II)-TiO<sub>2</sub> NR from the spectrum of DHNQ + Co(II)-TiO<sub>2</sub> NR, and at  $t > 40$  minutes most of the DHNQ was decomposed.

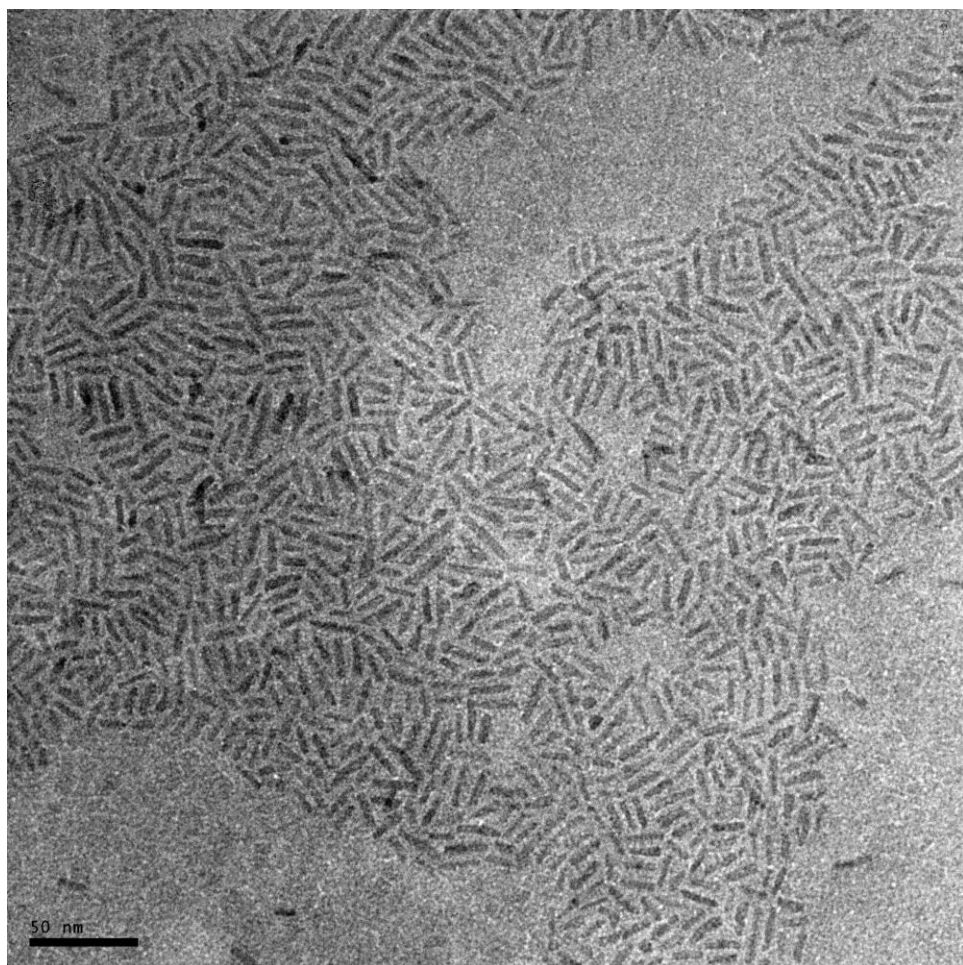


**Figure S17.** TEM data of Co(II)-TiO<sub>2</sub> NR sample recovered from the photocatalysis experiment.

### Calculation of dispersion of brookite $\text{TiO}_2$ NR.

We base our calculations on the findings reported by Gong and Selloni [2]. The nanorod geometry was assumed to be a cylinder with a diameter of 4.2 nm and a height of 20.9 nm. Therefore the volume of the cylinder is  $V = \pi r^2 h = 289.6 \text{ nm}^3$ .

The unit cell parameters of brookite are  $a = 5.456 \text{ \AA}$ ,  $b = 9.182 \text{ \AA}$ ,  $c = 5.143 \text{ \AA}$ ,  $\alpha = 90^\circ$ ,  $V = 0.2576 \text{ nm}^3$  and  $Z = 8$ . Therefore, there are 1124 brookite unit cells per nanorod and 8991  $\text{TiO}_2$  formula units per nanorod.

The brookite nanocrystal consists of the (210) facet, which has an area of 0.49  $\text{nm}^2$  per unit cell. The area of the (210) plane per unit cell is

$$c \left( \left( \frac{a}{2} \right)^2 + b^2 \right)^{1/2} \quad (1)$$

The surface area of the nanorod is  $2\pi rh + 2\pi r^2$ . The surface area of a single nanorod with a diameter of 4.2 nm and a height of 20.9 nm is 303.5  $\text{nm}^2$ .

There are 616 (210) 'unit planes' per nanorod, and each (210) 'unit plane' contains 4 Ti atoms. We estimate there are 2464 surface Ti atoms per nanorod.

The dispersion,  $D$  or the ratio of the number of surface Ti atoms to the total number of Ti atoms is  $2464/8991 = 0.274$ .

## References

1. Casavola, M.; Grillo, V.; Carlino, E.; Giannini, C.; Gozzo, F.; Pinel, E.F.; Garcia, M.A.; Manna, L.; Cingolani, R.; Cozzoli, P.D., *Nano Lett.*, **2007**, 7, 1386-1395.
2. Gong, X.-G.; Selloni, A., *Phys. Rev. B*, **2007**, 76, 235307.